BNL-105588-2014-TECH

BNL/SNS Technical Note No. 015;BNL-105588-2014-IR

Design of the NSNS Accumulator Ring Vacuum System

H. C. Hseuh

February 1997

Collider Accelerator Department

Brookhaven National Laboratory

U.S. Department of Energy

USDOE Office of Science (SC)

DISCLAIMER

DESIGN OF THE NSNS ACCUMULATOR RING VACUUM SYSTEM

BNL/NSNS TECHNICAL NOTE

NO. 015

H. C. Hseuh

February 12, 1997

ALTERNATING GRADIENT SYNCHROTRON DEPARTMENT
BROOKHAVEN NATIONAL LABORATORY
UPTON, NEW YORK 11973

DESIGN OF THE NSNS ACCUMULATOR RING VACUUM SYSTEM

The NSNS accumulator ring vacuum system is to provide a friendly environment for the transport of the beam during the one msec accumulation cycle. The operating pressure of the accumulator ring vacuum system will be 10^{-9} Torr and is needed to minimize the beam-residual gas ionization. The various beam-residual gas interactions are described in first section. The layout of the ring vacuum system, the design of the vacuum chambers, vacuum pumps and other hardware will be detailed in the successive sections.

I. Vacuum Requirement

The following beam-residual gas interactions are considered in assessing the required vacuum levels in the accumulator ring; the nuclear scattering, the multi coulomb scattering and the residual gas ionization. The nuclear scattering cross sections σ_n are proportional to the geometrical cross section of the target nucleus and are ~ $4*10^{-25}$ cm^2 and ~ $4*10^{-26}$ cm^2 for CO and H_2, respectively, which are the most common residual gases in a clean ultrahigh vacuum system. The beam loss due to nuclear scattering is given by $\Delta I / I = \int \beta\, c\, \sigma_n\, N\, dt$, with N being the residual gas density in the vacuum system. At the designed pressure of $1x10^{-9}$ Torr, N will be $7x10^{+7}$ atoms/cm^3. The resultant $\Delta I / I$ will be $\leq 3x10^{-10}$ over one msec.

The multi-Coulomb scattering causes the growth of the RMS beam size. The fraction of the increase in beam size can be calculated by[1] $\Delta\sigma_y / \sigma_y = \int k\, \beta_y\, N/ (p^2\, \epsilon)\, dt$, with σ_y the transverse beam dimension, $k = 1.085x10^{-23}$ (GeV/c)^2 m^3 sec^{-1}, β_y the betatron amplitude (<20m), p the momentum (= 1.696 GeV/c) and ε the transverse emittance (=120π mm.mrad?). The fraction of beam growth over one msec will be $<1x10^{-8}$ at a vacuum of $1x10^{-9}$ Torr.

The residual gas ionization sets the most stringent requirement on the vacuum levels. The ionization cross section depends on the types of the residual gas molecules and the velocity of the ionizing particles. The ionization cross sections of 1 GeV protons on H_2 and CO can be calculated using Bethe formula[2] and are $2x10^{-19}$ cm^2 and $9x10^{-19}$ cm^2, respectively. The newly created ions repelled by the beam wall potential will bombard the chamber wall and desorb molecules. The ionized electrons could be trapped in the potential well of the beam causing partial neutralization of the beam, or they could bombard the beam envelopes and liberate more secondary electrons.

I.A. Pressure Increase due to Ion Desorption

The ions will receive an energy corresponding to the potential at where they are created. For a pencil-like unbunched beam in a circular chamber, the potential is given by

$$V = (\lambda/2\pi\epsilon_o)\ \{r^2/2a^2 - \tfrac{1}{2} + \ln(r_o/a)\}$$

with r_o the radius of the vacuum chamber and a, the radius of the beam, and $\lambda = I/c$, the linear charge density. For the accumulator ring with I ~ 20 A at the end of one msec, and r_o/a ~5, an ion created at the edge of the beam will receive an energy of more than 1 keV. The beam wall potentials for a bunched beam have been derived previously.[3,4]. With a bunching factor of 0.33, the ions hitting the wall will have energy up to a few KeV. The ion desorption coefficient η, the number of gas molecules desorbed per incident ion, ranges from less than one for a baked and glow discharge cleaned surface to over 10 for an unbaked surface. If the rate of desorption is higher than the rate of removal, the pressure will rise gradually and leads to pressure instability. This could happen if η is large, the conductance of the chamber is small or the pumps are spaced too far apart.

The flow of the residual gas from x to x+dx along the chamber can be represented by

$$A\frac{dN(I,x)}{dt} = q + I\sigma_i N(I,x)\eta + C\frac{d^2N(I,x)}{dx^2}$$

with A the cross sectional area of the chamber, N(I,x) the gas density at location x (x = 0 midway between pumps), I the average current of the ring (=1/32th of the peak current), q the thermal outgassing rate per unit length of the chamber, σ_i the ionization cross section of the residual gas, and C the linear conductance of the chamber. Then the equilibrium gas density (at $t \to \infty$) without and with beam can be expressed by[5]

$$N(0,x) = q\left(\frac{L}{S} + \frac{L^2 - x^2}{2C}\right)$$

$$N(I,x) = \frac{q}{CW^2}\left[\frac{\cos Wx}{\cos WL - \frac{WC}{S}\sin WL} - 1\right]$$

with 2L the distance between pumps, 2S the pumping speed, and $W^2 = I\sigma_i\eta/C$. The gas density (and the pressure) will become infinite if the denominator in the above equation approaching zero. We have, hence, the pressure stability condition of ' **cosWL - (WC/S)*sinWL > 0** ' or ' **WL*tan(WL) < SL/C** '. For each set of S, L and C, there exists a critical value of $I*\eta$ when the pressure will increase exponentially and becomes unstable. The practical limit of η is decided by the allowable pressure rise in the presence of the beam, i.e., P(I,x)/P(0,x). In the accumulator ring design, a pressure increase of 10% is thought as not excessive and will be used in our calculation.

In the four arc regions of the accumulator ring, it is natural to position a pump at each arc halfcell therefore 2L equals 400cm, or 800cm in the worst scenario when every other pump fails. Other parameters of the halfcell chambers, such as the pumping speed 2S, the linear conductances, the ionization cross sections and the outgassing rates for H_2 and CO are listed in Table 1. The pressure distribution along the chambers without and with beam can then be calculated using the

above equations. The results are summarized in Table 1. The ratios of the pressures at x = 0 (mid point between pumps) and the corresponding η values for CO gas are plotted versus the fraction of the maximum WL values(a measure of the pressure instability limit) in Fig. 1 for a few scenarios. Owing to the high linear conductance of the chambers, the pressure gradient along the halfcell chamber length is less than 10% even when every other pump fails. The average pressure without beam will be $<1\times10^{-9}$ Torr and $<2\times10^{-10}$ Torr, respectively, for mild-baked and well-baked scenarios. To not exceed a pressure increase of 10% in the presence of the beam, the ion desorption yield η in the worst scenario(case B in Table 1) has to be < 4, which can be achieved on a clean and baked stainless steel or aluminum surface. No pressure instability due to ion desorption is expected in the arc chambers. The pressure distribution in the inj., extraction and RF straight sections will be determined by the design and processing of the components inside these chambers and will be modeled when the detail designs are completed.

Table 1. Pressure and allowable η in the NSNS arc chambers

Outgassing Rates, Linear Conductances and Ionization Cross Sections for H_2 and CO

	q (torr.*l*/sec.cm^2)	C (*l*.cm/sec)	σ_i(cm^2/sec)
H_2	2×10^{-12}	2.68×10^{5}	2×10^{-19}
CO(A&B)	1×10^{-12}	7.17×10^{4}	1×10^{-18}
CO(C&D)	2×10^{-13}	7.17×10^{4}	1×10^{-18}

Case A&B: mild baked and pumped by a 200 *l*/s sputter ion pump.
C&D: well baked and pumped by 1000 *l*/s titanium sublimation pump/sputter ion pump.
CO: represents the sum of residual gases other than H_2, ie. CH_4, CO, CO_2...

Calculated Pressures and Allowable Desorption Coefficients for Halfcell Chambers

	A(L=200 cm)	B(L=400 cm)	C(L=200 cm)	D(L=400 cm)
P(0,0)-H_2	2.9×10^{-10} Torr	6.0×10^{-10}	6.6×10^{-11}	1.5×10^{-10}
P(0,0)-CO	1.6×10^{-10}	3.6×10^{-10}	9.5×10^{-12}	2.7×10^{-11}
P(0,0)	4.5×10^{-10}	9.6×10^{-9}	7.6×10^{-11}	1.8×10^{-10}
P-avg	4.4×10^{-10}	9.2×10^{-9}	7.1×10^{-10}	1.6×10^{-10}
$\eta(H_2)$*	< 41	< 20	< 192	< 88
η(CO)*	< 7.9	< 3.7	< 31	< 12

*Allowable η values for a pressure increase of 10%, i.e., $P(I,0)/P(0,0) \leq 1.1$

I.B. The Effect of the Ionized Electron

The average energy of the newly ionized electrons will be at a few eV,[2] which is too low to escape the potential well of the beam if the beam is unbunched. For the bunched beam of the

accumulator ring, the bunch spacing is approximately 280 nsec which is long enough for the electrons generated in the drift space and in the dipole field to escape.[6] No accumulation of the electrons is expected here. Inside the quadrupole chambers, some electrons might be trapped and oscillating in the beam potential.[6] Beam position monitors located at the ends of the quadrupoles can be used as clearing electrodes. Operating at ~ 100 V, they will generate sufficient field to remove the trapped electrons.

Secondary electrons will be ejected from the chamber surface when bombarded by the ionized electrons. These electrons will be attracted by the next bunches and hit the wall liberating more electrons, the so called multipactoring effect. The secondary electron yields η of most technological materials increase with increasing energy then plateau around ~ 1 keV. With the exception of aluminum, the η values of the standard vacuum chamber materials[7] are < 1 if the energy of the electrons is less than 100 eV which is the case for the accumulator ring. With thorough insitu baking, the η of these materials[7] including aluminum can be reduced to below 1, thus avoiding multipactoring.

II. Ring Vacuum Layout

The accumulator ring has four arc regions and four long straight sections for injection, RF, collimators and extraction. The vacuum system will be divided into eight vacuum sectors isolatable with all metal pneumatic gate valves located at both ends of the arcs. The four arc vacuum sectors are ~ 32 m in length and the four straight vacuum sectors ~ 23m in length. A manually operated gate valve may be used to isolate the stripping foil mechanism at the injection straight section facilitating the foil changes.

The ring vacuum chambers can be grouped into two types; the halfcell chambers in the arcs and the various special chambers housing the inj., ext. RF and instrumentation components. The halfcell chambers consist of a combination chamber for dipole, quadruple, correctors and beam position monitors; and a short chamber for sextupole, bellows and pumping port. The chambers must provide a smooth and low impedance path for the image current of the beam. Tapered transition will be provided between the rectangular dipole cross section and the round quadruple cross section. RF finger contacts will be used inside the bellows. The pumping ports will be screened.

The usual materials for large UHV vacuum chambers are stainless steel and aluminum because of its good mechanical and magnetic properties, easiness to, weld and the low outgassing rates. No elastomer or organic material will be used. The vacuum chambers will consist of separate sections joined by demountable flange connections of Conflat type with aluminum or copper gaskets. These types of flanges and seals have proven their reliability in accelerator ultrahigh vacuum systems. In a few locations, such as injection, extraction and collimators, where the expected beam loss will be higher, quick demountable type flanges/seals will be used, therefore minimizing the radiation exposure during machine maintenance period. All the chambers will be chemically cleaned and assembled in a clean environment to minimize contamination. To achieve the low outgassing rates and the designed pressure, all the vacuum chambers and the components within are designed to be insitu bakeable.

II.A. Dipole and Quadruple Chambers

The layout of the arc halfcell chambers and the cross sections of the dipole and quadruple chambers are depicted in Fig. 2. The dipole chamber will have a rectangular cross section of 23cm(H) x 13cm(V) inner dimensions and will be curved with a bending angle of 15°. The length of the dipole chambers will be approximately 2 m long. There will be a tapered transition from the dipole chamber to the round quadruple/corrector chamber which has an I.D. of ~18 cm. The overall length of the dipole/quadruple chambers will be ~3.3 m. They will be made of A6061aluminum for its good mechanical properties and the ease of fabrication. The dipole chamber section can be made from machined plates e-beam welded or brazed together thus avoiding distortion usually associated with TIG welding of aluminum. To minimize the deflection of the chamber under the vacuum load, the wall thickness of the dipole chambers will be ~ 15 mm. The quadruple sections will be made of seamless aluminum pipes. The tapered transition can be machined from a solid aluminum block. Explosive bonded aluminum-to-stainless Conflat flanges will be used at both ends of the chamber. After thorough chemical cleaning, these three sections, the beam position monitor housing and the flanges will be jointed together with an automatic welder on a precision fixture. The completed chambers will be wrapped with heating jackets before installation into the 'opened' magnets. Gaps of ~ 5 mm between the chamber and the magnet poles will be sufficient for the heating jackets to insulate the magnets from the 150 C chambers during insitu bake.

II.B. The Pump Chambers

The short chambers of the halfcells contain the bellows and the pumpout port. These chambers will be round with I.D. of 18cm, length of ~0.7 m and made of 316L stainless steel. One end of the short chambers will be tapered to match the rectangular cross section of the dipole chambers. To minimize the radiation induced stress corrosion, the thin wall bellows will be made of inconel. Internal sliding contacts will be provided to shield the bellows. The pump port with 8" Conflat flange will be screened with ~80% transparency for evacuation. One side port of 2-3/4" Conflat flange will be provided on the pump chamber for other vacuum hardware such as vacuum gauges, residual gas analyzers and roughing valve.

II.C. The Long Straight Section Chambers

The halfcells in the four straight sections will consist of round pipes for the quadruples and special chambers housing the r.f. cavities, collimators, injection and extraction equipments. The quadruple pipes with I.D. of 28cm will be fabricated of aluminum. The design of the special chambers will follow closely with the design of the special components to ensure that both vacuum and beam requirements are met. As in the arc chambers, they will be all metal or ceramics and insitu bakeable. No elastomers or organic materials are allowed. To minimize the residual radiation, aluminum will be the preferred material for the chambers in the straight sections. Large bakeable and quick demountable flanges and seals such as the Helicoflex type will be developed for some of these chambers.

III. Pumpdown, Insitu Bakeout and Conditioning

The eight ring vacuum sectors will be isolatable with all metal gate valves. The gate valves are interlocked by the vacuum sensors upstream and downstream of the valves therefore protecting the ring from catastrophic failure. They also allow the repair and modification of components without venting the other regions. At additional cost, the gate valves can be fabricated with RF contact figures. Mobile roughing carts connected to the roughing ports at the pump chambers will be used to pump down the vacuum sectors and to maintain the vacuum during insitu bake. Each roughing cart will consist of a dry mechanical pump, a turbomolecular pump, electropneumatic isolation valve and vacuum gauges. The roughing cart will be valved out and removed from the tunnel when roughing and bakeout is complete and high vacuum pumps activated.

Each vacuum sector and the entire vacuum sector is to be baked insitu to 150°C for aluminum chambers and 250°C for stainless steel sections. All the chambers will be wrapped with heating jackets and instrumented with thermocouples. The bakeout will be carried out with mobile bakeout carts fashioned after AGS Booster bakeout carts. Industrial programmable logic controllers and PC-based software will control and monitor the bakeout process.

The high linear conductance provided by the large aperture of the halfcell chambers makes distributed pumping less important. Lumped pumps will be used. As detailed earlier, one sputter ion pump of 200 ℓ/sec every 4 m (length of the arc halfcells) will be sufficient to maintain the 10^{-9} Torr vacuum and meet the pressure stability requirement. At this operating pressure, the lifetime of the sputter ion pumps will exceed 20 years. The ion pump current which is proportional to pressure can be used to measure the pressure distribution around the ring. In addition, titanium sublimation pumps of ~ 1000 ℓ/sec each can be used in augment of the sputter ion pumps and reduce the average pressure into low 10^{-10} Torr range. The titanium sublimation pump will be fitted into the housing of the sputter ion pump saving the precious space in the tunnel. The pumping requirement in the four straight sections will be modeled with the detailed design of these regions. The designed vacuum can be achieved by positioning large pumps adjacent to the components with high outgassings.

IV. Vacuum Instrumentation and Control

Two sets of pirani and cold cathode gauges will be installed at each vacuum sector as primary vacuum gauges. The sputter ion pump current will give a more detailed pressure profile around the ring. A residual gas analyzer will also be installed at each vacuum sector and will provide a quick analysis of the partial pressures around the ring. Due to the potential high radiation level in the tunnel, all the electronics including gauge controllers and pump power supplies will be located at the service buildings. These devices with local and remote capabilities can be operated through front panels and will communicate with the vacuum programmable logic controllers(PLC) through IEEE488 links for remote monitoring and control. The PLCs with its own application software will provide the interlock logic and the on-line menu for the operation of the sector gate valves. Ethernet type link will connect the PLC to the VME crate and the front end computer for monitoring, logging and control of the

vacuum devices. Redundant hardwired interlock will be provided for the beam permit link and to abort the beam during vacuum faults.

References

[1] G. Guignard, **CERN 77-10**, p33, June, 1977.
[2] Y. Baconnier, Proceeding CERN Accel. School, **CERN 85-19**, pp267-300, Nov. 1985.
[3] J.C. Herrera, BNL-20325, **ISA-75-7**, June 1975.
[4] H.J. Halama, BNL-17820, **AADD, 73-7**, April, 1973.
[5] E. Fischer and K. Zankel, **CERN-ISR-VA/73-52**, Nov., 1973.
[6] A.G. Ruggerio, NSNS Tech. Note No. **8**, Jan. 1997.
[7] R. Calder and A.G.Mathewson, Vacuum, **29**, 53(1979)
[8] C. Pai, Private communication, Jan., 1997

Fig. 1. Allowable desorption Yields and Pressure Increase in NSNS Arc Chambers versus the fraction of W*L

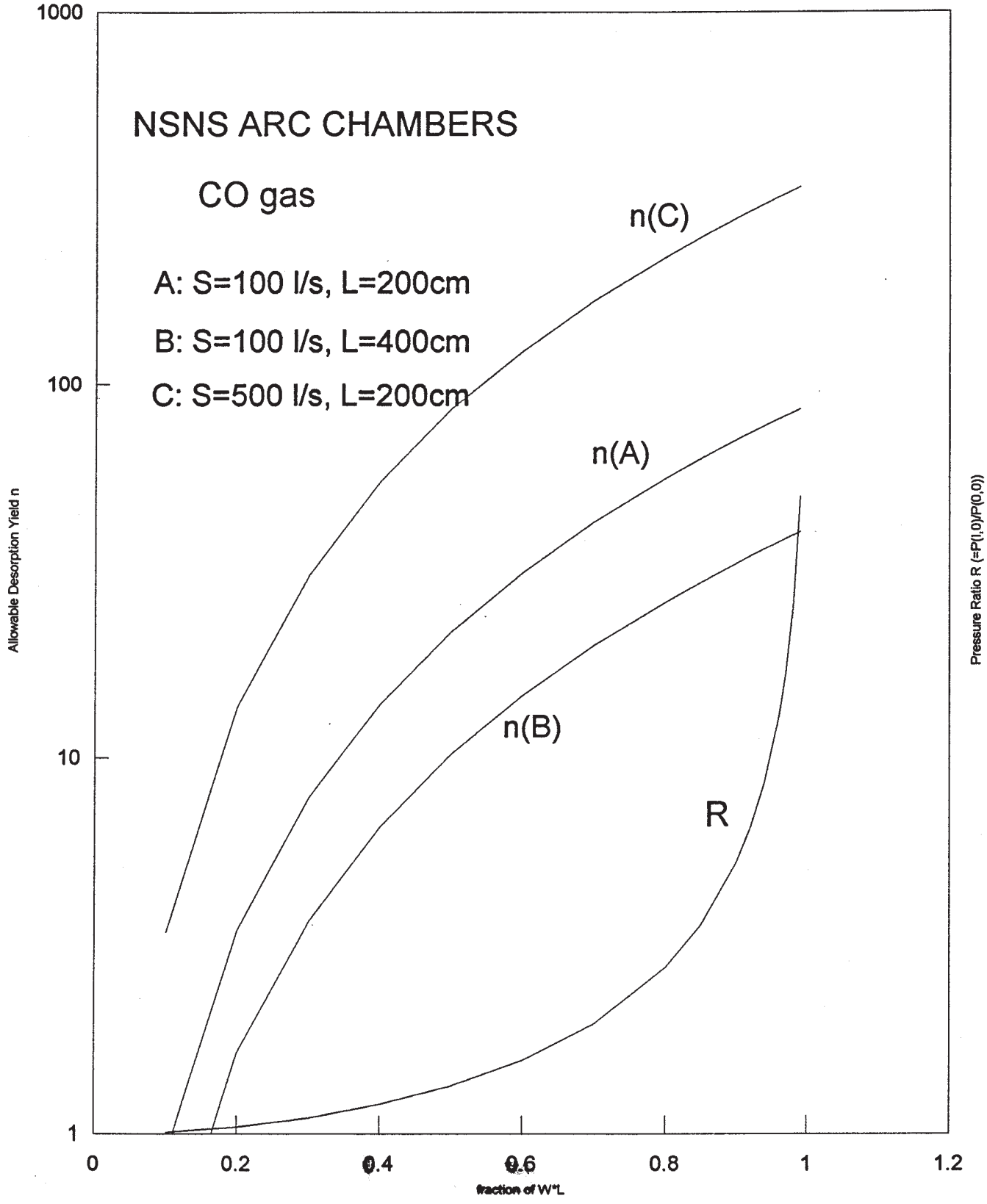

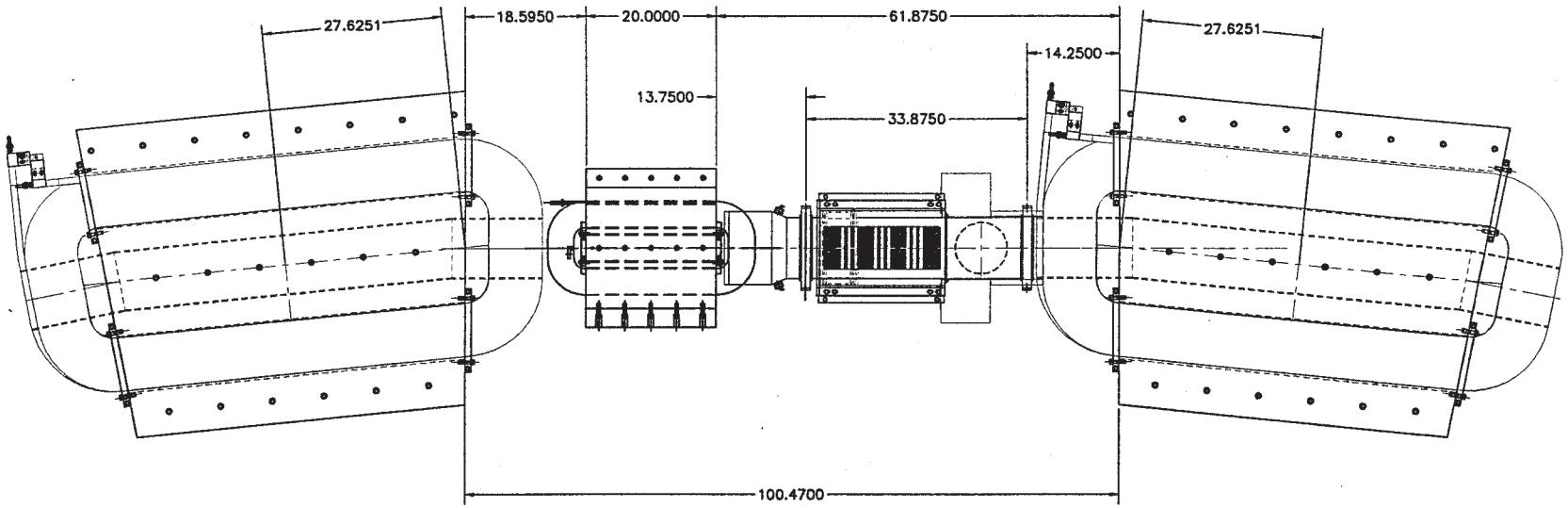

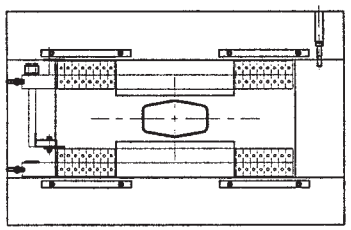

END VIEW
DIPOLE MAGNET

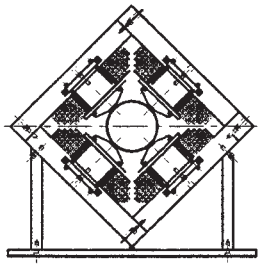

END VIEW
QUADRUPOLE MAGNET

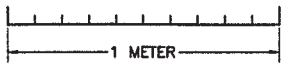

Fig. 2 - Halfcell Layout and Chamber Cross Sections.